American Journal of Physics and Applications
2019; 7(2): 34-42
http://www.sciencepublishinggroup.com/j/ajpa
doi: 10.11648/j.ajpa.20190702.11
ISSN: 2330-4286 (Print); ISSN: 2330-4308 (Online)

Study on the Use of Silicon Drift Detector to Get Information on Light Emitted by Luminescent Materials

Murielle Béranger

Process Department, Trixell, Moirans, France

Email address:
Murielle.beranger@trixell-thalesgroup.com

To cite this article:
Murielle Béranger. Study on the Use of Silicon Drift Detector to Get Information on Light Emitted by Luminescent Materials. *American Journal of Physics and Applications.* Vol. 7, No. 2, 2019, pp. 34-42. doi: 10.11648/j.ajpa.20190702.11

Received: January 23, 2019; **Accepted**: March 5, 2019; **Published**: March 21, 2019

Abstract: Energy dispersive X-Ray detectors are among the most common tools installed on scanning electron microscopes and, as they are sensitive to light, they can be used to get panchromatic cathodoluminescence information. This article presents practical considerations about the parameters to choose to obtain a good cathodoluminescence signal on a silicon drift detector. Probe current is the most important but other parameters of electron microscope and energy dispersive X-Ray detector are also explored. Filament brightness, if not fixed, influences the number of electrons incident on the sample and modifies cathodoluminescence response. Beam voltage and working distance must be adapted to the sample and to the electron microscope geometry. Acquisition and shaping times are important parameters for spectrum quality: the high sensitivity of silicon drift detector to light allows the use of low acquisition times and high shaping times. As cathodoluminescent materials are mostly high band gap materials, charge effects can influence their response and the size of the acquisition area must be carefully chosen. The influence of all these parameters is studied through two scintillating materials. Some examples of application are described to show the potential of this method. They include localization of luminescent particles, a demonstration of the effect of strong electron beam on a needle of material and the characterization of light emitted by a structural defect in a scintillator material.

Keywords: Cathodoluminescence, Energy Dispersive X-Ray Detector, Silicon Drift Detector, Luminescent Material

1. Introduction

Energy dispersive X-Ray (EDX) detectors are among the most common tools installed on scanning electron microscopes (SEM). The first employed detectors possessed Si (Li) sensors, which needed liquid nitrogen cooling. In the middle of 2000s came silicon drift detectors, which work at higher temperature and higher count rates [1-3]. During the last 20 years, silicon drift detectors were improved [4-5]: increase of sensor active area [6], new geometries decreasing detector – specimen distance [7-8] and new materials for the window or windowless detectors [4, 9-10] allowed to improve the spatial resolution and the detection of low energy X-rays. EDX detectors are made from silicon, a material in which X-ray photons but also visible light can create electron-hole pairs, which are further collected to give the useful signal. So EDX detectors can be used to get information on the light emitted by samples, a task usually done by sophisticated cathodoluminescence equipment. However, few studies have been conducted on this subject.

In their article, P. F. Smet et al. studied the behavior of a Si-Li detector exposed to the light of luminescent BaAl2S4: Eu+ films [11]. They found that the effect of light on the EDX detector is a peak at very low energy. The throughput count rate of this peak varies exponentially with the probe current of the SEM. The behavior of a silicon drift detector (SDD) is somewhat different [12]. The count rate increases first with the probe current, then reaches a maximum and decreases. It looks like the electronics are not able anymore to detect the incoming photons when the quantity of emitted light is too high.

The aim of this work is to explore further the possibility of performing cathodoluminescence with a SDD, by searching for the parameters that can influence the signal and giving some examples of application. But before beginning, the working of a SDD is explained and a few useful terms are defined.

2. The Working of a SDD

The core of a SDD is made from a slice of high purity silicon on which a complex set of concentric electrodes is deposited [2, 4, 13]. Each incoming X-ray (or visible photon) creates electron hole pairs in the silicon. The electrodes generate a field gradient which drifts down the electrons to a small collection electrode. A Field Effect Transistor (FET) preamplifier converts the charge accumulated at the anode in a voltage step proportional to the energy of the incoming X-ray. The output from the preamplifier is a voltage ramp where each voltage step corresponds to an incoming photon. As charge built up regularly due to incoming X-rays, it is restored to prevent the saturation of the preamplifier. The voltage signal is analyzed by a pulse processor, which realizes shaping and noise reduction. Voltage noise is reduced by signal averaging over a time called process time or shaping time. The longer the process time, the lower the noise: with a longer process time, the resolution is higher as the X-Ray peak energy is measured more precisely. However there is a drawback to long shaping times. When two photons arrive very close one from another, in a time interval lower than the process time, the measurement is rejected. The time corresponding to rejected measurements is called dead time, it is usually expressed as a percentage of the total counting time. The longer the process times the higher the dead times. This dependence of resolution on shaping time is no longer present in newer detectors [4]. Count rate can be calculated for each peak of the spectrum: the throughput count rate is the count rate of X-ray or light pulses which are successfully processed by the detector electronics, while the input count rate takes into account all pulses which arrive in the detector, no matter if they are processed or rejected [14]. The input count rate is more representative of the sample behavior as it takes into account all the photons emitted by the sample.

3. Equipment and Materials

All the experiments were conducted in a Leo 440 SEM. The SDD is an Inca X-Act (supplier Oxford) with a 10mm2 chip. To account for possible variations in the emission of the tungsten filament, the filament current and the column are settled on a cobalt standard and the number of counts in the L-peak of cobalt is measured before each set of measurements. On scintillator samples, a new area is selected on the surface for each measurement. Two scintillators for medical imaging are used in this study: cesium oxide activated by thallium (CsI:Tl) and Gadox [15, 16]. CsI:Tl scintillators are manufactured at Trixell. Micro-columns (or needles) of CsI:Tl are obtained by evaporation on an aluminum substrate. This scintillator emits visible light centered on 550nm, which corresponds to green color and is well adapted to photodiodes absorption. Gadox is bought from the supplier MCC. It is formed by luminescent gadolinium oxysulfure grains doped with terbium and embedded in a polymer matrix. Gadox emits a line spectrum due to a transition located on the terbium atom. The spatial resolution of CsI:Tl is higher than the one of Gadox because of its micro-columnar structure which acts as a light guide. For the study of the influence of SEM and EDX parameters, scintillator surface is polished to get a flat surface and avoid shadowing effects; CsI: Tl is cut along the needles axis before polishing. As both scintillators are insulating materials, they are discharged by a thin layer of carbon evaporated on their surface.

4. Cathodoluminescence in Practice

When facing a new sample, the microscopist must ask itself the following question: which parameters should I choose on my equipment to get the best signal? These parameters can be divided in two sets: parameters linked with the SEM like beam voltage, beam current or working distance, and parameters useful for EDX spectrum acquisition (acquisition or process time for example). These parameters must be adapted to the observations to be done and to the nature of the sample.

4.1. SEM Parameters

4.1.1. Filament and Probe Current

The most influential parameter for cathodoluminescence is the quantity of electrons incident on the sample. This parameter depends on the microscope settings: brightness of the gun, acceleration voltage V, settings of condensing lenses, diameter of the final aperture.

The current density J on the sample can be related to the current density J_0 at the gun level by the Langmuir formula [17]:

$$J=J_0 \frac{eV}{kT} \alpha^2 \quad (1)$$

where e is the electron charge, k the Boltzmann constant, T the temperature and α the half opening angle of the beam. In the Leo S440 microscope, the probe current is calculated with the beam voltage V, the current of the two condensing lenses and the diameter of the final diaphragm. This probe current takes into account all the elements of the Langmuir formula except the current density at the gun level, which is not supposed to vary.

For a non-luminescent sample like the aluminum foil of figure 1, the probe current does not influence the count rate in the low energy peak, as this peak is due to electronic noise. When a sample emits light, the count rate of this peak increases with probe current and the steepness of the curve is related to the quantity of emitted light. In the example of figure 1, the CsI:Tl scintillator emits more light than Gadox material and reaches its maximum at a lower probe current value. The maximum value of the count rate is about the same for both luminescent samples. Only the first part of the curve, where the count rate increases with probe current, is useful. In this part, the count rate N in the low energy peak can be described by an exponential function of the probe current I:

$$N = A\, e^{KI} \quad (2)$$

The exponential term K is proportional to the quantity of

emitted light [12].

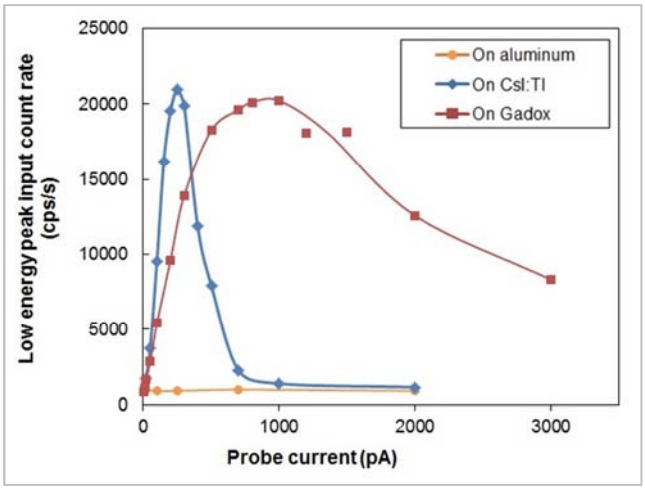

Figure 1. *Evolution of the low energy peak count rate with probe current.*

The major problem of the analyst is to find the good probe current range for its analysis. To look completely at the influence of current density on cathodoluminescence, the current density J_0 at the gun level has to be taken into account. The Leo 440 microscope possesses a thermionic tungsten filament; such filaments emit electrons when they are heated at a very high temperature by a current I_f flowing through them. The current density is given by the Richardson-Dushman formula [17]:

$$J_0=\frac{4\pi mek^2}{h^3}\ T^2\ e^{\frac{-\varphi}{kT}} \quad (3)$$

where m is the electron mass, h the Planck constant and φ the work function of the filament material.

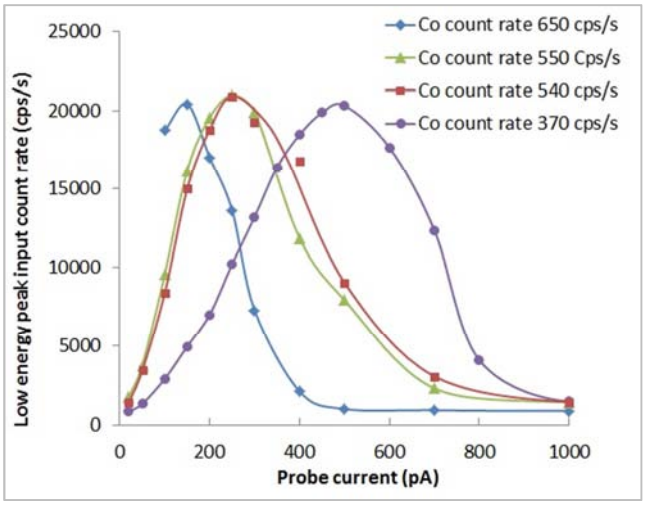

Figure 2. *Evolution of the low energy peak count rate with probe current for different filament brightness.*

J_0 increases very rapidly with temperature; temperature is given by the current applied to the filament to heat it and by the diameter of the filament. With time, atoms evaporate from the filament and its diameter decreases: the filament current must be decreased to avoid a premature breaking. J_0 is not very stable and can vary during a long session and with filament age. To evaluate the influence of the filament emission, a spectrum is acquired on a cobalt reference: the count rate in the Co peaks varies linearly with the number of incident electrons and is representative of the filament brightness.

The influence of the gun brightness is illustrated in figure 2, where cathodoluminescence curves are acquired on a CsI:Tl sample for different filament currents. For a brighter filament, the count rate in the low energy peak increases more rapidly with probe current and the maximum of the cathodoluminescence curve arises at a lower probe current. The sample seems to have a higher sensitivity. Curves acquired at about the same filament condition superimpose. A solution to set free from the variations of the filament brightness is to use the input count rate in one of the X-ray peaks of the sample instead of the probe current, as they are proportional. As an example, figure 3 shows that the curves acquired with different filament conditions superimpose when traced against the input count rate in the iodine 4 keV peak. This solution is efficient for studies of samples having the same chemical composition but not for samples of different nature, like CsI and Gadox. In this case, probe current must be used and special care must be taken to have the same count rate on a reference sample at the beginning and at the end of each session to be able to compare the samples from day to day and ensure that the filament brightness did not change during the session.

4.1.2. Beam Voltage

The choice of the beam voltage value is strongly dependent on the nature of the sample because the voltage value and the density of the sample give the penetration depth of the electrons in the material. A reduction in beam voltage leads to a lower volume analyzed and a better spatial resolution, as illustrated in reference [6] in pure iron. Monte Carlo simulations can be used to calculate the volume of interaction, but also some author have proposed formula to express the distance R traveled by the electrons as a function of the beam energy E_0. The one of Kayana and Obayama gives [18]:

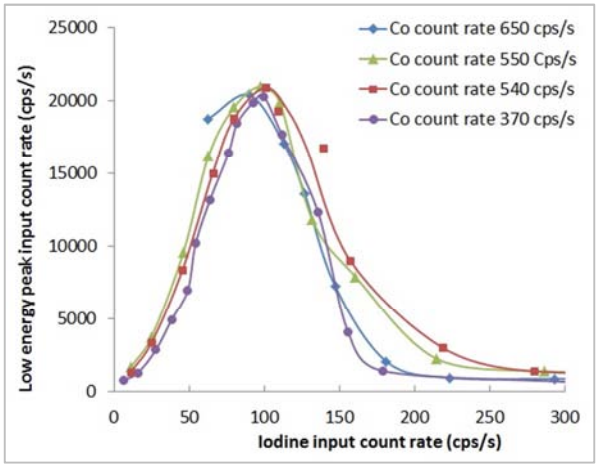

Figure 3. *Evolution of the low energy peak count rate with iodine X-ray peak for different filament brightness.*

Table 1. *Distance traveled by electrons in CsI as a function of beam voltage.*

E0 (keV)	R (µm)
5	0.3
10	1.1
15	2.1
20	3.4
25	4.9
30	6.7

$$R = 0.0276A\frac{E_0^{1.67}}{\rho Z^{0.89}} \quad (4)$$

ρ is the material density, A its molar mass and Z its atomic number. Table 1 gives the value of R for different beam energies in CsI. As CsI is a heavy material with a high density, the distance traveled by electrons is low, in the micrometer range or even less. Electrons penetration depth is always lower than the distance R, as electrons do not travel on a straight line in the matter. The energy value chosen for CsI:Tl is 20 keV to allow the electrons to penetrate enough in the material. Gadox is an inhomogeneous material, made from luminescent grains of oxysulfure of gadolinium embedded in a polymer matrix. The luminescent material is heavy and a 20 KeV energy is also well adapted. Moreover, both these scintillator materials are insulators and they are discharged by a thin layer of carbon. Inside the material, an electrical field builds up due to trapped charges under the surface. Electron trajectories are further deflected and penetration depth is even lower than its theoretical value calculated without charge effects [19].

In the first part of this article, for the study of the influence of SEM and EDX parameters, flat samples were obtained by mechanical polishing. The upper layer of the samples is affected by this process and in this layer luminescence can be modified by defects created by polishing [20]. This phenomenon is also in favor of a high value for beam voltage.

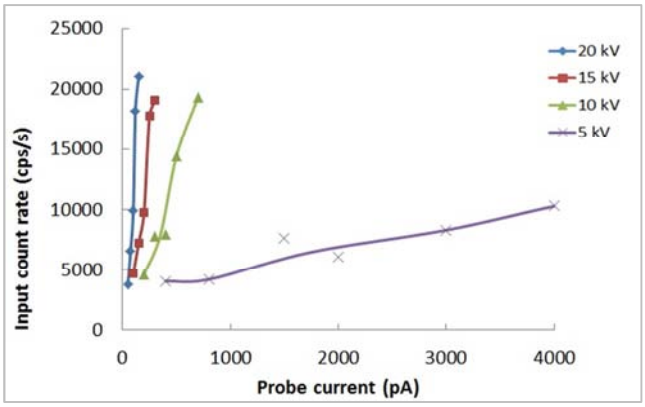

Figure 4. *Evolution of the low energy peak count rate with probe current as a function of beam voltage.*

The cathodoluminescence behavior of a CsI:Tl sample subjected to different beam voltages is illustrated in figure 4. The low energy peak count rate increases with voltage beam, indicating that light quantity emitted by the sample is higher. Note that the reference signal on cobalt is also slightly higher when beam voltage increases. At 5 kV, penetration depth of the electrons is too low, the quantity of light emitted by the sample is very small and the low energy peak count rate increases very slowly with probe current. Similar studies were conducted with cathodoluminescence systems to evaluate the depth of sub-surface damage after polishing. For example, in reference [20], panchromatic cathodoluminescence images of a GaN substrate were taken at different beam voltages between 5kV and 20kV and the depth of the damaged area after polishing was estimated at 1.48µm. For our CsI:Tl sample, a damaged area of the order of magnitude of one micron or less could explain the big difference between the cathodoluminescence curves at 5 kV and at higher voltages.

4.1.3. Working Distance

The working distance WD is the distance between the sample and the objective lens. The optimum value of WD, i.e. the value which gives the highest count rate on X-Ray peaks, depends on the detector size and the geometry of the microscope. For the SDD used in his study, optimum value is about 23 mm. A Gadox sample is used to check if the limit of detection is the same for X-Rays and visible light. The K coefficient of several areas of the Gadox is calculated as a function of WD (see figure 5). At 15 mm and below, neither light nor X-rays is able to reach the detector. All higher values give a good detection of X-rays and light. There are some variations in the calculated K value because the homogeneity of Gadox material is not very good.

4.2. X-ray Acquisition Parameters

Two parameters have to be set to acquire a spectrum: acquisition time and process time (or shaping time).

4.2.1. Process Time

The influence of process time on the shape of the low energy peak is the same than its influence on X-ray peaks in the Inca detector: a low process time deteriorates the energy resolution, the peak being broader [14]. This fact is illustrated in figure 6, where cathodoluminescence signal is acquired for different shaping times on a CsI:Tl sample. The low energy peaks present the same width for shaping times between 16 and 100 µs but the peak is much broader for the lowest shaping time of 4 µs. In such a short time, the energy of the peak cannot be measured precisely.

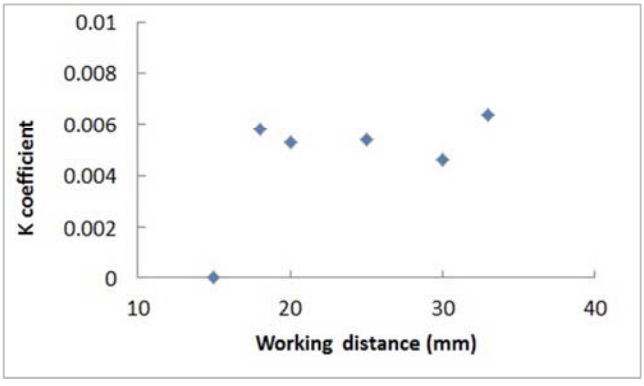

Figure 5. *Evolution of K coefficient with working distance.*

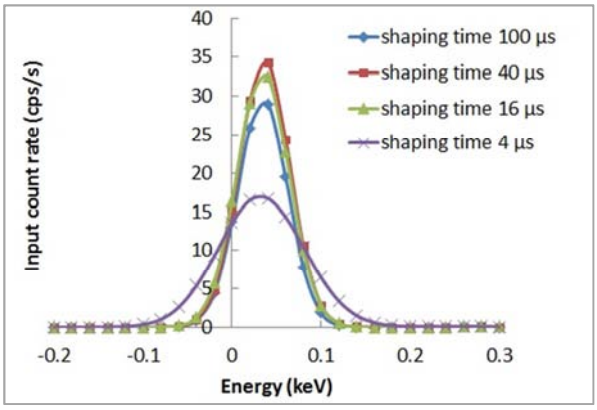

Figure 6. *Shape of low energy peak.*

Dead time is known to increase slowly with probe current for X-ray peaks; it is higher for higher process times. For a highly luminescent sample like CsI:Tl, the probe current range used for cathodoluminescence is low and the count rate in the X-ray peaks is almost negligible in front of the count rate of the low energy peak; so the evolution of dead time with probe current follows the one of the low energy peak, increasing with probe current and reaching a maximum before decreasing. In the example of figure 7, the dead time value stays lower than 6% for the 4 µs shaping time but it reaches 37% at its maximum for the highest process time.

The influence of shaping time on the count rate of the low energy peak is different from the one of X-ray peaks. For X-ray peaks, the input count rate does not depend on the process time. The throughput count rate is lower for higher process times because of the increase of the dead time [4, 14]. The behavior is different for cathodoluminescence. The throughput count rate is about the same for all shaping times (see figure 8-9). Note that because of variations in the filament brightness, the curves are plotted as a function of iodine count rate. The input count rate does not depend significantly on the process time in the first part of the cathodoluminescence curve. But the maximum value is lower for lower shaping times. As the energy of the cathodoluminescence peak is very low, one can imagine that this peak is less detected with the lowest shaping times.

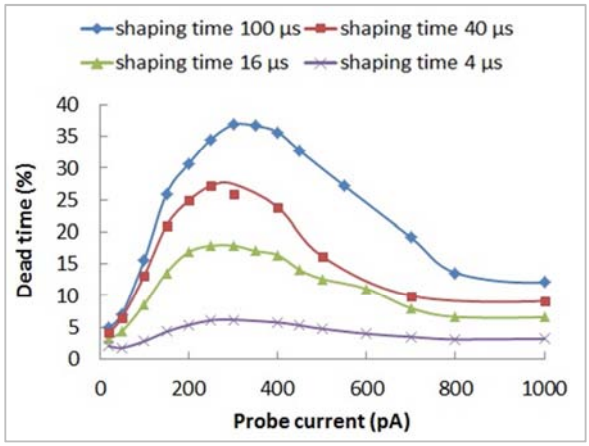

Figure 7. *Influence of probe current on dead time.*

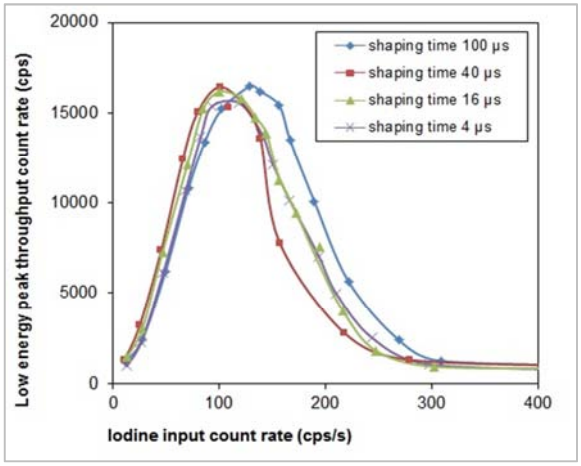

Figure 8. *Throughput count rate for different shaping times.*

4.2.2. Acquisition Time

The value chosen for the acquisition time (or real time) depends on the number of counts expected in the spectrum. Increasing the acquisition time gives more counts at the cost of waiting. But long acquisition times can present some drawbacks: higher possibility of pollution under the electron beam and deterioration of the sample if it is fragile. For a luminescent sample, the count rate in the low energy peak is high and cathodoluminescence information can be collected in a few seconds, unlike X-ray information.

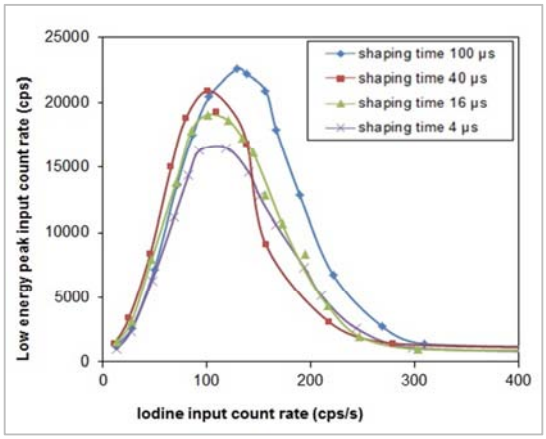

Figure 9. *Input count rate for different shaping times.*

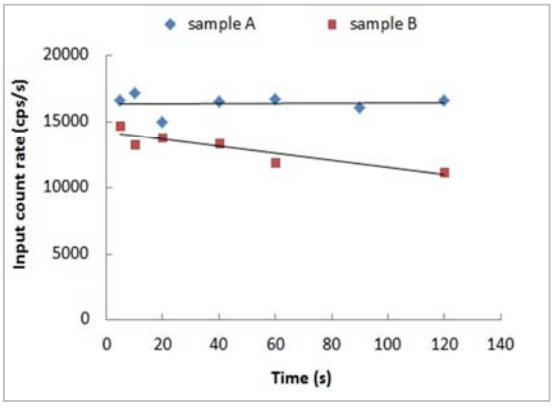

Figure 10. *Influence of acquisition time on count rate.*

The low energy peak count rate should not depend on the acquisition time for a sample that is not affected by the electron beam. Figure 10 presents the count rate as a function of acquisition time for two CsI:Tl samples which show some difference in chemical composition and possess different sensitivities : sample A emits more light than sample B. The probe current value was set a little lower than the one which gives the maximum count rate. The count rate in the low energy peak of sample A is stable whereas the one of sample B decreases with increasing acquisition times. Sample B seems to be more sensitive to the electron beam than sample A. The phenomenon of time dependence of cathodoluminescence intensity is frequently observed in semiconductors or wide bandgap materials. For example, in natural quartz crystals, the cathodoluminescence intensity was shown to rapidly increase and then decrease for higher irradiation times [21]. In undoped or Si-doped GaN, cathodoluminescent peaks can increase or decrease with excitation time depending on temperature and injection current [22]. Proposed explanations include surface and bulk charge effects, absorption – desorption of surface contamination, surface annealing, modification of the luminescence mechanism or modification of luminescence intensity due to temperature effects.

4.2.3. Size of the Acquisition Area

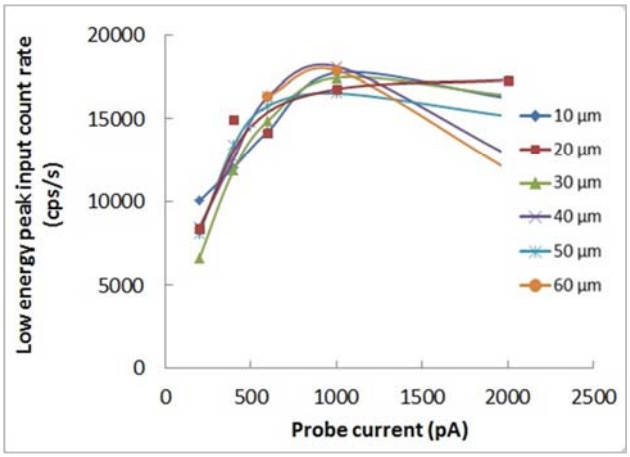

Figure 11. *Influence of acquisition size on Gadox.*

The last parameter that the microscopist has to set up is the size of the area used to acquire the spectrum. This parameter was tested on Gadox in the range of 10 to 60 µm (below 10 µm this material is not considered as homogeneous); it was also tested on CsI:Tl from 2.5 µm to 60 µm. For a sample which is insensitive to the electron beam, the size of the acquisition area should not have any effect on the low energy peak count rate. It is the case for the Gadox sample and for the CsI:Tl sample A, down to 10 µm (figures 11, 12, 13). For sample A at 2.5 µm and for sample B, it is clearly observed that the slope of the count rate curve is lower for smaller acquisition areas and that the maximum occurs at a higher probe current. The K coefficient deduced from these curves decreases with the size of the acquisition area. It is 40% lower at 10µm than at 60 µm in sample B (see figure 14). It was checked that the shape of the area (square or rectangular) has no effect on count rate. Similar effects were demonstrated in reference [22]: GaN cathodoluminescence bands were found to be strongly dependent on electron beam spot size, magnification and raster scan, because these parameters have a strong influence on excitation density. The authors' conclusion is that cathodoluminescence comparison of different specimens should be undertaken only when the spectra are collected under identical SEM operating conditions.

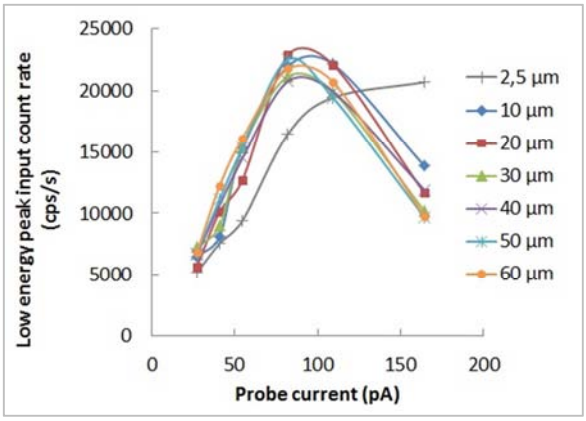

Figure 12. *Influence of acquisition size on CsI:Tl – A.*

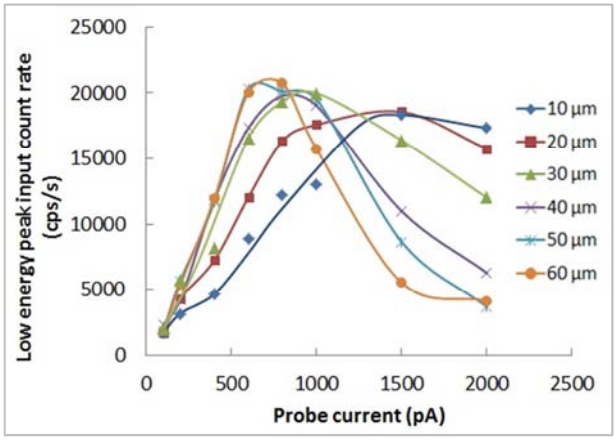

Figure 13. *Influence of acquisition size on CsI:Tl – B.*

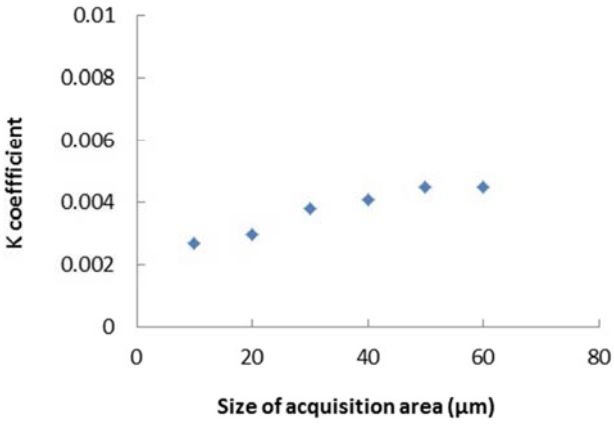

Figure 14. *K coefficient on Cs:Tl – B.*

4.3. Conclusion SEM and EDX Parameters

As shown in precedent paragraphs, the most important parameter for cathodoluminescence is the quantity of electrons incident on the sample surface. This quantity of electrons is proportional to the probe current, provided that the filament brightness is constant. The count rate in one of the X-ray peaks of the sample can be used to normalize curves obtained with different filament brightness values, when working with samples which have the same chemical composition. Filament voltage should be chosen as a function of the sample material, taking into consideration penetration depth of the incident electrons, possible charge effects and sample preparation. The high sensitivity of SDD to light allows short acquisition times and low probe currents. Working distance and shaping time can be set at the same value for cathodoluminescence and for X-ray studies. If the sample is sensitive to the electron beam, variations of count rate with acquisition time and the size of the acquisition area can occur: in this case only spectra acquired in the same conditions should be compared.

5. Examples of Application

This section gives some examples of application of cathodoluminescence using a SDD on CsI:Tl scintillators. As explained in the last section, the energy of the beam is kept high, at 20keV, to obtain a significant penetration of the electrons in the material. WD is set at 23mm. The process time is fixed at 100 µs to get a high resolution for the peaks. For each example, the acquisition time and the size of the acquisition area are kept constant.

5.1. Particle Localization

The first application example concerns the acquisition time. Cathodoluminescence using a SDD was used to localize CsI:Tl particles among several other particles collected on a carbon adhesive. In this case, the behavior of the luminescent material is known (see paragraph 4) and the useful probe current value is chosen at 100pA. An area where several particles are present is selected and cartography is acquired with only 10 cycles, for a little more than 10s (see figure 15). The CsI:Tl particle is clearly identified in the low energy peak image, even with such a short time, while no signal was detected in the cesium or iodide X-Ray images. Similar work of detection of luminescent particles was proposed in reference [23], cathodoluminescence images were taken at 10kV with a low scanning rate of 10s/frame to visualize decay times of the phosphors.

5.2. Electron Beam Sensitivity

CsI:Tl can be sensitive to the electron beam at very high currents and cathodoluminescence is used to demonstrate this sensitivity. A secondary electron image and a cathodoluminescence image (i.e. low energy peak cartography) are acquired at 100 pA on a single needle of CsI:Tl. The emission of light is homogeneous over the length of the needle. Then a severe electron irradiation is performed in the center of the needle with a probe current of 5 nA during 60s. The cathodoluminescence image acquired just after his electron irradiation show a much darker area in the center of the needle, while no modification is observed in the secondary electron image (see figure 16). EDX spectra show no increase of the carbon peak, indicating that the sample was not contaminated by carbon during the irradiation. This darker area could be due to some charge effect; in this case the spectrum would be cut before 20 keV in the irradiated area. The high energy cut arises around 18 keV for the spectra in irradiated and non-irradiated areas, indicating that there is no important charge effect and that the charge effect is the same in both areas. Quantifying the modification of light emission in the irradiated area is somewhat difficult. On a first needle, spectra were acquired during 30s at different probe currents between 50 and 500 pA. However the non-irradiated area appeared to be darker after the acquisition of the spectra, indicating that the electron beam might have had an effect on the luminescence. The same measurement was repeated on another needle, with an acquisition time of 10s and currents between 20 and 300 pA ; after the acquisition of the spectra, no significant contrast was observed under the electron beam. The K coefficient in the irradiated area was found to be 2 times lower than the one in the non-irradiated area. This result is given only to show the interest of the cathodoluminescence method, and a more complete work should be done to study the sensitivity of CsI:Tl under the electron beam.

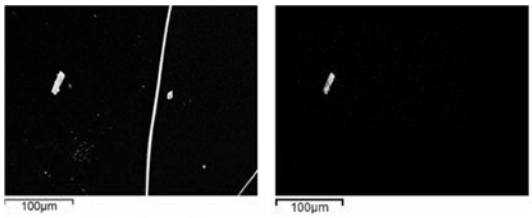

Figure 15. *Example of application, particle localization.*

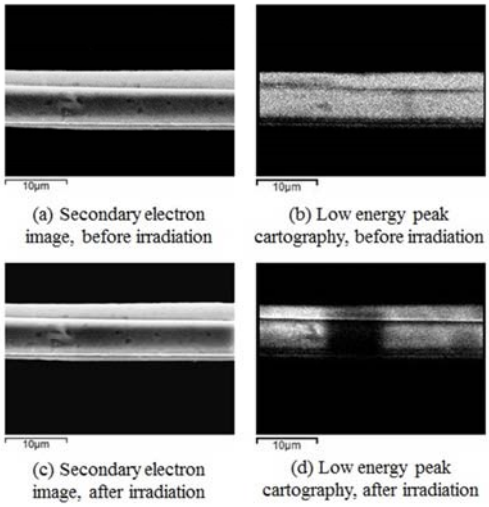

Figure 16. *Influence of electron beam sensitivity.*

5.3. Defect Study

Cathodoluminescence can be used to study locally the influence of defects on luminescence. Figure 17 displays a small growth defect, i.e. an area where the CsI:Tl needles do not have the same diameter than in the rest of the sample. Cathodoluminescence images are acquired at different probe currents: the gray level of the defect is about the same than the one of the rest of the sample and the probe current at which there is no more detection of luminescence is the same. Spectra at different probe currents between 20 and 75 pA are used to calculate the K coefficient: its value is 0.046 for the defect and 0.048 for the non-defective area, so it can be concluded that the defect emits the same quantity of light than the rest of the sample.

6. Conclusion

This article presents a study of cathodoluminescence using a SDD. SEM and EDX parameters influencing the measurement are explored. The most important parameter for cathodoluminescence is probe current. The useful range of probe current values is found with the acquisition of a few spectra. When a sample emits a significant quantity of light, the count rate in the low energy peak is high, allowing the use of low acquisition times: in practice, looking for this probe current range does not take a long time. When the luminescent material is known, this time is even shorter. For the study of scintillators, filament voltage is chosen as a function of the material, to get a sufficient penetration of electrons and to avoid artefacts due to sample preparation. Working distance is not a sensitive parameter. Shaping time can be chosen with the same considerations than for X-rays, and the high sensitivity of SDD to light at low excitation level permits the use of long shaping times. As shown through the examples of application, this technique gives the opportunity to all laboratories equipped with a basic system (SEM and SDD) to get information on light emitted by luminescent materials.

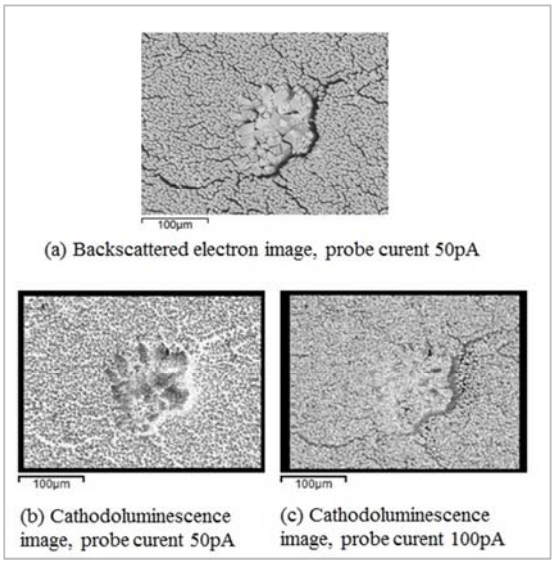

Figure 17. *Defect study in CsI:Tl.*

References

[1] P. Lechner, C. Fiorini, R. Hartmann, J. Kemmer, N. Krause et al., "Silicon drift detectors for high count rate X-ray spectroscopy at room temperature", NIM vol. A458, pp. 281-287, 2001.

[2] P. Lechner, C. Fiorini, A. Longoni, G. Lutz, A. Pahlke et al., "Silicon drift detectors for high resolution, high count rate X-ray spectroscopy at room temperature" Advances in X-ray Analysis Vol. 47, pp. 53-58, 2004.

[3] D. E. Newbury, "X-ray spectrometry and spectrum image mapping at output count rates above 100 kHz with a silicon drift detector on a scanning electron microscope", Scanning vol. 27, pp. 227–239, 2005.

[4] T. Nylese, J. Rafaelsen, "Improvements in SDD Efficiency – From X-ray Counts to Data", Microscopy Today, vol. 25-2, pp. 46–53, 2017.

[5] A. Liebel, A. Schöning, A. Bechteler, K. Hermenau, K. Heinzinger, L. Strüder, A. Niculae1, H. Soltau1, "Silicon Drift Detectors in Electron Microscopy – An Over 20 Year History with a Bright Future", Microsc. Microanal. 24 - Suppl 1, pp. 796-797, 2018.

[6] S. Burgess, X. Li, J. Holland, "High spatial resolution energy dispersive X-ray spectrometry in the SEM and the detection of light elements including lithium", Microscopy and Analysis vol. 27-4, pp. 8-13, May 2013.

[7] R. Terborg, A. Kaeppel, B. Yu, M. Patzschke, T. Salge, M. Falke, "Advanced Chemical Analysis Using an Annular Four-Channel Silicon Drift Detector", Microsc. Today vol. 25-2, pp. 30-35, 2017.

[8] N. Brodusch, H. Demers, R. Gauvin, "X-Ray Imaging with a Silicon Drift Detector Energy Dispersive Spectrometer" in "Field Emission Scanning Electron Microscopy", Springer: Singapore, Briefs in Applied Sciences and Technology, 2018. pp. 67-84.

[9] S. Burgess, J. Sagar, J. Holland, X. Li, F. Bauer, "Ultra-Low kV EDS – A New Approach to Improved Spatial Resolution, Surface Sensitivity, and Light Element Compositional Imaging and Analysis in the SEM", Microsc. Today vol. 25-2, pp. 20-28, 2017.

[10] J. Rafaelsen, T. Nylese, M. Bolorizadeh, V. Carlino,"Windowless, Silicon Nitride window and Polymer window EDS detectors: Changes in Sensitivity and Detectable Limits", Microsc. Microanal. 21- Suppl 3, pp. 1645-19646, 2015.

[11] P. F. Smet, J. E. Van Haecke, D. Poelman, "Spatially resolved cathodoluminescence of luminescent materials using an EDX detector", Journal of Microscopy Vol. 231-1, pp. 1-8, July 2008.

[12] M. Béranger, "Use of a silicon drift detector for cathodoluminescence detection", Microelectronics Reliability vol. 55, 1569–1573, 2015.

[13] Oxford Instruments, "Silicon drift detectors explained", Application note, 2012, pp. 2-27.

[14] A. Kenik, "Evaluating the performance of a commercial silicon drift detector for X-ray microanalysis", Microsc. Today vol. 19-3, pp. 40–46, 2011.

[15] P. Lecoq, A. Annenkov, A. Gektin, M. Korzhik, C. Pedrini, Inorganic Scintillators for Detector Systems : physical principles and crystal engineering, Springer: Berlin, 2006, pp. 54–59.

[16] G. Blasse, B. C. Grabmaier, Luminescent Materials, Springer-Verlag: Berlin Heidelberg, 1994, pp. 40–45.

[17] G. R. Leiker, "Design and construction of a high power electron gun", M. S. Thesis, faculty of Texas, pp. 6-17, 1984.

[18] T Koshikawa and R Shimizu, "A Monte Carlo calculation of low-energy secondary electron emission from metals", J. Phys. D Appl. Phys. 7, pp. 1303-1315, 1974.

[19] W. Vanderlinde, "Scanning electron microscopy", in "Microelectronics failure analysis", Ed. The Electronic Device Failure Analysis Society Desk Reference Committee, 2004, pp. 559-573.

[20] K. Y. Lai, M. A. L. Johnson, T. Paskova, A. D. Hanser, K. Udwary, E. A. Preble, and K. R. Evans," Cathodoluminescence evaluation of subsurface damage in GaN substrate after polishing", Phys. Status Solidi C 6- S2, pp. S325–S328, 2009.

[21] F. Bresse, G. Remondz., B. Akamatsu, "Cathodoluminescence Microscopy and Spectroscopy of Semiconductors and Wide Bandgap Insulating Materials", Mikrochim. Acta Suppl. 13, pp. 135-166, 1996.

[22] M. R. Phillips, H. Telg, S. O. Kucheyev, Olaf Gelhausen, M. Toth, "Cathodoluminescence Efficiency Dependence on Excitation Density in n-Type Gallium Nitride", Microsc. Microanal. 9, pp. 144–151, 2003.

[23] Paul Harris, Daniel den Engelsen, Terry Ireland, George Fern and Jack Silver, "Cathodoluminescence studies of phosphors in a scanning electron microscope", Journal of Physics: Conference Series 619, pp. 1-4, 2015.